

ECL: Class-Enhancement Contrastive Learning for Long-tailed Skin Lesion Classification

Yilan Zhang¹, Jianqi Chen¹, Ke Wang¹, and Fengying Xie^{1*}

Image Processing Center, School of Astronautics, Beihang University, Beijing 100191,
China
xfy_73.buaa.edu.cn

Abstract. Skin image datasets often suffer from imbalanced data distribution, exacerbating the difficulty of computer-aided skin disease diagnosis. Some recent works exploit supervised contrastive learning (SCL) for this long-tailed challenge. Despite achieving significant performance, these SCL-based methods focus more on head classes, yet ignoring the utilization of information in tail classes. In this paper, we propose class-Enhancement Contrastive Learning (ECL), which enriches the information of minority classes and treats different classes equally. For information enhancement, we design a hybrid-proxy model to generate class-dependent proxies and propose a cycle update strategy for parameters optimization. A balanced-hybrid-proxy loss is designed to exploit relations between samples and proxies with different classes treated equally. Taking both “imbalanced data” and “imbalanced diagnosis difficulty” into account, we further present a balanced-weighted cross-entropy loss following curriculum learning schedule. Experimental results on the classification of imbalanced skin lesion data have demonstrated the superiority and effectiveness of our method. The codes can be publicly available from <https://github.com/zy1buaa/ECL.git>.

Keywords: Contrastive learning · Dermoscopic image · Long-tailed classification.

1 Introduction

Skin cancer is one of the most common cancers all over the world. Serious skin diseases such as melanoma can be life-threatening, making early detection and treatment essential [3]. As computer-aided diagnosis matures, recent advances with deep learning techniques such as CNNs have significantly improved the performance of skin lesion classification [6,7]. However, as a data-hungry approach, CNN models require large balanced and high-quality datasets to meet the accuracy and robustness requirements in applications, which is hard to suffice due to the long-tailed occurrence of diseases in the real-world. Long-tailed problem is usually caused by the incidence rate and the difficulty of data collection. Some

* Corresponding author

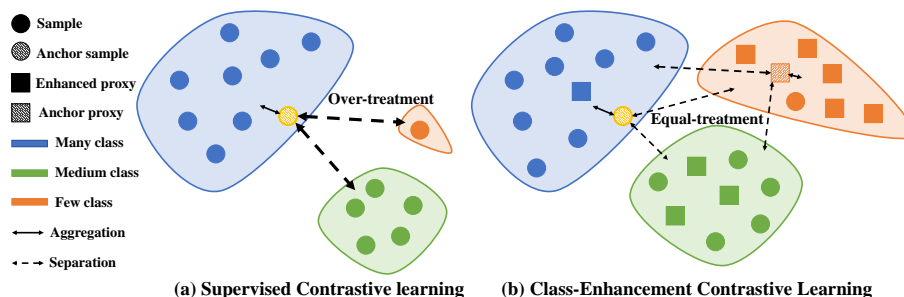


Fig. 1. Comparison between SCL (a) and ECL (b). In SCL, head classes are over-treated leading to optimization concentrating on head classes. By contrast, ECL utilizes the proxies to enhance the learning of tail classes and treats all classes equally according to balanced contrastive theory [23]. Moreover, the enriched relations in samples and proxies are helped for better representations.

diseases are common while others are rare, making it difficult to collect balanced data [12]. This will cause the head classes to account for the majority of the samples and the tail classes only have small portions. Thus, existing public skin datasets usually suffer from imbalanced problems which then results in class bias of classifier, for example, poor model performance especially on tail lesion types.

To tackle the challenge of learning unbiased classifiers with imbalanced data, many previous works focus on three main ideas, including re-sampling data [1,17], re-weighting loss [14,2,21] and re-balancing training strategies [9,22]. Re-sampling methods over-sample tail classes or under-sample head classes, re-weighting methods adjust the weights of losses on class-level or instance-level, and re-balancing methods decouple the representation learning and classifier learning into two stages or assign the weights between features from different sampling branches [20]. Despite the great results achieved, these methods either manually interfere with the original data distribution or improve the accuracy of minority classes at the cost of reducing that of majority classes [11,12].

Recently, contrastive learning (CL) methods pose great potential for representation learning when trained on imbalanced data [13]. Among them, supervised contrastive learning (SCL) [10] aggregates semantically similar samples and separates different classes by training in pairs, leading to impressive success in long-tailed classification of both natural and medical images [15]. However, there still remain some defects: (1) Current SCL-based methods utilize the information of minority classes insufficiently. Since tail classes are sampled with low probability, each training mini-batch inherits the long-tail distribution, making parameter updates less dependent on tail classes. (2) SCL loss focuses more on optimizing the head classes with much larger gradients than tail classes, which means tail classes are all pushed farther away from heads [23]. (3) Most methods only consider the impact of sample size (“imbalanced data”) on the classification

accuracy of skin diseases, while ignoring the diagnostic difficulty of the diseases themselves (“imbalanced diagnosis difficulty”).

To address the above issues, we propose a class-Enhancement Contrastive Learning method (ECL) for skin lesion classification, differences between SCL and ECL are illustrated in Fig.1. For sufficiently utilizing the tail data information, we attempt to address the solution from a proxy-based perspective. A proxy can be regarded as the representative of a specific class set as learnable parameters. We propose a novel hybrid-proxy model to generate proxies for enhancing different classes with a reversed imbalanced strategy, *i.e.*, the fewer samples in a class, the more proxies the class has. These learnable proxies are optimized with a cycle update strategy that captures original data distribution to mitigate the quality degradation caused by the lack of minority samples in a mini-batch. Furthermore, we propose a balanced-hybrid-proxy loss, besides introducing balanced contrastive learning (BCL) [23]. The new loss treats all classes equally and utilizes sample-to-sample, proxy-to-sample and proxy-to-proxy relations to improve representation learning. Moreover, we design a balanced-weighted cross-entropy loss which follows a curriculum learning schedule by considering both imbalanced data and diagnosis difficulty.

Our contributions can be summarized as follows: (1) We propose an ECL framework for long-tailed skin lesion classification. Information of classes are enhanced by the designed hybrid-proxy model with a cycle update strategy. (2) We present a balanced-hybrid-proxy loss to balance the optimization of each class and leverage relations among samples and proxies. (3) A new balanced-weighted cross-entropy loss is designed for an unbiased classifier, which considers both “imbalanced data” and “imbalanced diagnosis difficulty”. (4) Experimental results demonstrate that the proposed framework outperforms other state-of-the-art methods on two imbalanced dermoscopic image datasets and the ablation study shows the effectiveness of each element.

2 Methods

The overall end-to-end framework of ECL is presented in Fig. 2. The network consists of two parallel branches: a contrastive learning (CL) branch for representative learning and a classifier learning branch. The two branches take in different augmentations $T^i, i \in \{1, 2\}$ from input images X and the backbone is shared between branches to learn the features $\tilde{X}^i, i \in \{1, 2\}$. We use a fully connected layer as a logistic projection for classification $g(\cdot) : \tilde{\mathcal{X}} \rightarrow \tilde{\mathcal{Y}}$ and a one-hidden layer MLP $h(\cdot) : \tilde{\mathcal{X}} \rightarrow \mathcal{Z} \in \mathbb{R}^d$ as a sample embedding head where d denotes the dimension. \mathcal{L}_2 -normalization is applied to \mathcal{Z} by using inner product as distance measurement in CL. Both the class-dependent proxies generated by hybrid-proxy model and the embeddings of samples are used to calculate balanced-weighted cross-entropy loss, thus capturing the rich relations of samples and proxies. For better representation, we design a cycle update strategy to optimize the proxies’ parameters in hybrid-proxy model, together with a curriculum learning schedule for achieving unbiased classifiers. The details are introduced as follows.

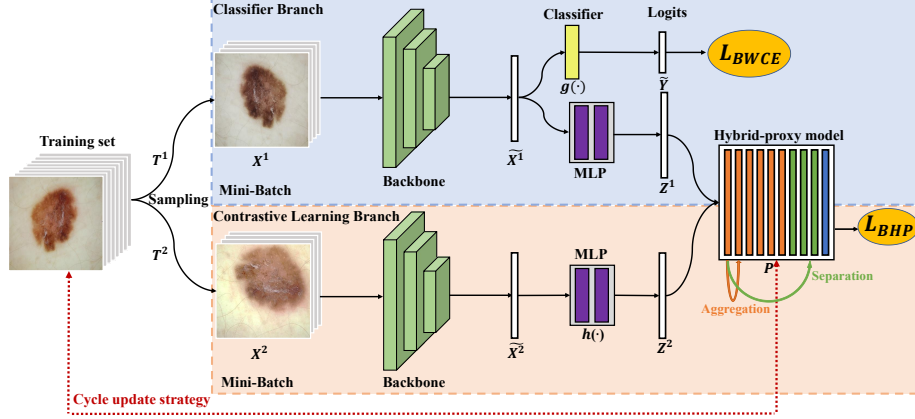


Fig. 2. Overall framework of the proposed ECL. ECL has two branches for classifier learning (guided by balanced-weighted cross-entropy loss L_{BWCE}) and contrastive learning (guided by balanced-hybrid-proxy loss L_{BHP}). Proxies in hybrid-proxy model are generated by a reserve imbalanced way (see Section 2.1) to strengthen the information of minority classes in a mini-batch.

2.1 Hybrid-Proxy Model

The proposed hybrid-proxy model consists of a set of class-dependent proxies $\mathcal{P} = \{p_k^c | k \in \{1, 2, \dots, N_c^p\}, c \in \{1, 2, \dots, C\}\}$, C is the class number, $p_k^c \in \mathbb{R}^d$ is the k -th proxy vector of class c , and N_c^p is the proxy number in this class. Since samples in a mini-batch follow imbalanced data distribution, these proxies are designed to be generated in a reversed imbalanced way by giving more representative proxies of tail classes for enhancing the information of minority samples. Let us denote the sample number of class c as N_c and the maximum in all classes as N_{max} . The proxy number N_c^p can be obtained by calculating the imbalanced factor $\frac{N_{max}}{N_c}$ of each class:

$$N_c^p = \begin{cases} 1 & N_c = N_{max} \\ \lfloor \frac{N_{max}}{10N_c} \rfloor + 2 & N_c \neq N_{max} \end{cases} \quad (1)$$

In this way, the tail classes have more proxies while head classes have less, thus alleviating the imbalanced problem in a mini-batch.

As we know, a gradient descent algorithm will generally be executed to update the parameters after training a mini-batch of samples. However, when dealing with an imbalanced dataset, tail samples in a batch contribute little to the update of their corresponding proxies due to the low probability of being sampled. So how to get better representative proxies? Here we propose a cycle update strategy for the optimization of the parameters. Specifically, we introduce the gradient accumulation method into the training process to update proxies asynchronously. The proxies are updated only after a finished epoch that all data has been processed by the framework with the gradients accumulated. With such a

Algorithm 1: Training process of ECL.

Input: Training set X , validation set X_{val} , training epochs E , iterations T , batch size B , learning rate lr , stages in balanced-weighted cross-entropy loss E_2

- 1 Initialize *model* parameters θ and hybrid-proxy model \mathcal{P} parameters ϕ
- 2 **for** e in E **do**
- 3 **for** t in T **do**
- 4 Getting a batch of samples $\{x_i^{(1,2)}, y_i\}_B$
 $\{z_i^{(1,2)}\}_B, \{\tilde{y}_i\}_B = \text{model}(\{x_i^{(1,2)}\}_B)$
 // curriculum learning
- 5 **if** $e > E_2$ **then**
- 6 $Loss(\theta, \phi) = \lambda L_{BHP}(\{z_i^{(1,2)}\}_B, \mathcal{P}) + \mu L_{BWCE}(\{y_i, \tilde{y}_i\}_B, f^e)$
- 7 **else**
- 8 $Loss(\theta, \phi) = \lambda L_{BHP}(\{z_i^{(1,2)}\}_B, \mathcal{P}) + \mu L_{BWCE}(\{y_i, \tilde{y}_i\}_B)$
- 9 $grad_{\theta}^t = \nabla_{\theta} Loss(\theta), grad_{\phi}^t = \nabla_{\phi} Loss(\phi)$ // calculate gradients
- 10 $\theta \leftarrow \theta - lr * grad_{\theta}^t$ // update parameters θ of *model*
- 11 $\phi \leftarrow \phi - \sum_t^T lr * grad_{\phi}^t$ // update parameters ϕ of \mathcal{P}
- 12 **if** $e > E_2$ **then**
- 13 $f^e = \text{Validate}(\text{model}, X_{val})$

strategy, tail proxies can be optimized in a view of whole data distribution, thus playing better roles in class information enhancement. Algorithm 1 presents the details of the training process.

2.2 Balanced-Hybrid-Proxy Loss

To tackle the problem that SCL loss pays more attention on head classes, we introduce BCL and propose balanced-hybrid-proxy loss to treat classes equally. Given a batch of samples $\mathcal{B} = \{(x_i^{(1,2)}, y_i)\}_B$, let $\mathcal{Z} = \{z_i^{(1,2)}\}_B = \{z_1^1, z_2^2, \dots, z_B^1, z_B^2\}$ be the feature embeddings in a batch and B denotes the batch size. For an anchor sample $z_i \in \mathcal{Z}$ in class c , we unify the positive image set as $z^+ = \{z_j | y_j = c, j \neq i\}$. Also for an anchor proxy p_i^c , we unify all positive proxies as p^+ . The proposed balanced-hybrid-proxy loss pulls points (both samples and proxies) in the same class together, while pushes apart samples from different classes in embedding space by using dot product as a similarity measure, which can be formulated as follows:

$$L_{BHP} = -\frac{1}{2B + \sum_{c \in C} N_c^p} \sum_{s_i \in \{\mathcal{Z} \cup \mathcal{P}\}} \frac{1}{2B_c + N_c^p - 1} \sum_{s_j \in \{z^+ \cup p^+\}} \log \frac{\exp(s_i \cdot s_j / \tau)}{E} \quad (2)$$

$$E = \sum_{c \in C} \frac{1}{2B_c + N_c^p - 1} \sum_{s_k \in \{\mathcal{Z}_c \cup \mathcal{P}_c\}} \exp(s_i \cdot s_k / \tau) \quad (3)$$

where B_c means the sample number of class c in a batch, τ is the temperature parameter. In addition, we further define \mathcal{Z}_c and \mathcal{P}_c as a subset with the label c of \mathcal{Z} and \mathcal{P} respectively. The average operation in the denominator of balanced-hybrid-proxy loss can effectively reduce the gradients of the head classes, making an equal contribution to optimizing each class. Note that our loss differs from BCL as we enrich the learning of relations between samples and proxies. Sample-to-sample, proxy-to-sample and proxy-to-proxy relations in the proposed loss have the potential to promote network’s representation learning. Moreover, as the skin datasets are often small, richer relations can effectively help form a high-quality distribution in the embedding space and improve the separation of features.

2.3 Balanced-Weighted Cross-Entropy Loss

Taking both “imbalanced data” and “imbalanced diagnosis difficulty” into consideration, we design a curriculum schedule and propose balanced-weighted cross-entropy loss to train an unbiased classifier. The training phase are divided into three stages. We first train a general classifier, then in the second stage we assign larger weight to tail classes for “imbalanced data”. In the last stage, we utilize the results on the validation set as the diagnosis difficulty indicator of skin disease types to update the weights for “imbalanced diagnosis difficulty”. The loss is given by:

$$L_{BWCE} = -\frac{1}{B} \sum_{i=1}^B w_i CE(\tilde{y}_i, y_i) \quad (4)$$

$$w_i = \begin{cases} 1 & e < E_1 \\ \left(\frac{C/N_c}{\sum_{c \in C} 1/N_c}\right)^{\frac{e-E_1}{E_2-E_1}} & E_1 < e < E_2 \\ \left(\frac{C/f_c^e}{\sum_{c \in C} 1/f_c^e}\right)^{\frac{e-E_2}{E-E_2}} & E_2 < e < E \end{cases} \quad (5)$$

where w denotes the weight and \tilde{y} denotes the network prediction. We assume f_c^e is the evaluation result of class c on validation set after epoch e and we use f1-score in our experiments. The network is trained for E epochs, E_1 and E_2 are hyperparameters for stages. The final loss is given by $Loss = \lambda L_{BHP} + \mu L_{BWCE}$ where λ and μ are the hyperparameters which control the impact of losses.

3 Experiment

3.1 Dataset and Implementation Details

Dataset and Evaluation Metrics. We evaluate the ECL on two publicly available dermoscopic datasets ISIC2018[4,18] and ISIC2019[4,5,18]. The 2018

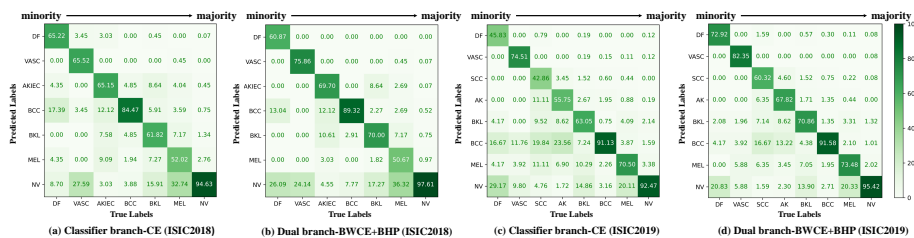


Fig. 3. The results of confusion matrix illustrate that ECL obtains great performance on most classes especially for minority classes.

dataset consists of 10015 images in 7 classes while a larger 2019 dataset provides 25331 images in 8 classes. The imbalanced factors $\alpha = \frac{N_{max}}{N_{min}}$ of the two datasets are all > 50 (ISIC2018 58.30 and ISIC2019 53.87), which means that skin lesion classification suffers a serious imbalanced problem. We randomly divide the samples into the training, validation and test sets as 3:1:1.

We adopt five metrics for evaluation: accuracy (Acc), average precision (Pre), average sensitivity (Sen), macro f1-score (F1) and macro area under curve (AUC). Acc and F1 are considered as the most important metrics in this task.

Implementation Details. The proposed algorithm is implemented in Python with Pytorch library and runs on a PC equipped with an NVIDIA A100 GPU. We use ResNet50 [8] as backbone and the embedding dimension d is set to 128. We use SGD as the optimizer with the weight decay $1e-4$. The initial learning rate is set to 0.002 and decayed by cosine schedule. We train the network for 100 epochs with a batch size of 64. The hyperparameters E_1 , E_2 , τ , λ , and μ are set to 20, 50, 0.01, 1, and 2 respectively. We use the default data augmentation strategy on ImageNet in [8] as T_1 for classification branch. And for CL branch, we add random grayscale, rotation, and vertical flip in T_1 as T_2 to enrich the data representations. Meanwhile, we only conduct the resize operation to ensure input size $224 \times 224 \times 3$ during testing process. The models with the highest Acc on validation set are chosen for testing. We conduct experiments in 3 independent runs and report the standard deviations in the supplementary material.

3.2 Experimental Results

Quantitative Results. To evaluate the performance of our ECL, we compare our method with 10 advanced methods. Among them, focal loss [14], LDAM-DRW [2], logit adjust [16], and MWNL [21] are the re-weighting loss methods. BBN [22] is the methods based on re-balancing training strategy while Hybrid-SC [19], SCL [10,15], BCL [23], TSC [13] and ours are the CL-based methods. Moreover, MWNL and SCL have been verified to perform well in the skin disease classification task. To ensure fairness, we re-train all methods by rerun their released codes on our divided datasets with the same experimental settings.

Table 1. Comparison results on ISIC2018 and ISIC2019 datasets.

Methods	ISIC2018					ISIC2019				
	Acc	Sen	Pre	F1	AUC	Acc	Sen	Pre	F1	AUC
CE	83.89	69.56	73.62	70.34	94.81	82.41	67.02	77.32	70.90	95.37
Focal Loss	84.19	68.78	76.69	71.38	94.76	82.05	64.55	75.93	68.84	94.82
LDAM-DRW	84.20	71.74	74.65	71.98	95.22	82.29	68.08	74.61	70.84	95.65
Logit Adjust	84.15	71.54	71.78	70.77	95.55	81.93	68.94	69.12	68.64	95.17
MWNL	84.90	73.90	76.94	74.92	96.79	84.10	74.83	75.81	75.08	96.61
BBN	85.57	74.96	72.40	72.79	93.72	83.43	71.78	78.37	74.42	95.10
Hybrid-SC	86.30	73.93	75.84	74.34	96.33	84.69	70.90	76.87	73.27	96.67
SCL	86.13	70.40	80.88	74.27	96.56	84.60	70.90	81.66	75.07	96.21
BCL	84.92	72.87	71.15	71.57	95.61	83.47	73.52	74.17	73.50	95.95
TSC	85.94	73.35	77.77	74.94	95.83	84.75	71.89	79.81	75.13	95.84
Ours	87.20	73.01	83.44	76.76	96.55	86.11	76.57	83.22	79.46	96.78

We also confirmed that all models have converged and choose the best eval checkpoints. The results are shown in Table 1. It can be seen that ECL has a significant advantage with the highest level in most metrics on two datasets. Noticeably, our ECL outperforms other imbalanced methods by great gains, e.g., 2.56% in Pre on ISIC2018 compared with SCL and 4.33% in F1 on ISIC2019 dataset compared with TSC. Furthermore, we draw the confusion matrixes after normalization in Fig. 3, which illustrate that ECL has significantly improved most of the categories, from minority to majority.

Table 2. Ablation study on ISIC2019 dataset.

Methods(ISIC2019)	Proxies	Acc	Sen	Pre	F1	AUC
Classifier branch-CE	HPM	82.41	67.02	77.32	70.90	95.37
Classifier branch-BWCE	HPM	82.69	67.95	77.32	71.65	95.37
Dual branch-CE+BHP	HPM	85.49	73.35	81.61	76.76	96.52
Dual branch-BWCE+BHP	2 proxies per-class	85.52	74.03	81.46	77.22	96.53
Dual branch-BWCE+BHP	3 proxies per-class	85.36	73.49	83.00	77.53	96.74
Dual branch-BWCE+BHP	4 proxies per-class	85.79	74.09	82.03	77.42	96.53
Dual branch-BWCE+BHP	w/o cycle strategy	85.65	73.48	83.00	77.40	96.65
	HPM	86.11	76.57	83.22	79.46	96.78

Ablation Study. To further verify the effectiveness of the designs in ECL, we conduct a detailed ablation study shown in Table S2 (the results on ISIC2018 are shown in supplementary material Table S2). First, we directly move the contrastive learning (CL) branch and replaced the balanced-weighted cross-entropy (BWCE) loss with cross-entropy (CE) loss. We can see from the results that adding CL branch can significantly improve the network’s data representation

ability with better performance than only adopting a classifier branch. And our BWCE loss can help in learning a more unbiased classifier with an improvement of 1.94% in F1 compared with CE on ISIC2019. Then we train the ECL w/o cycle update strategy. The overall performance of the network has declined compared with training w/ the strategy, indicating that this strategy can better enhance proxies learning through the whole data distribution. In the end, we also set the proxies' number of different classes equal to explore whether the classification ability of the network is improved due to the increase in the number of proxies. With more proxies, metrics fluctuate and do not increase significantly. However, the result of using proxies generated by reversed balanced way in hybrid-proxy model (HPM) outperforms equal proxies in nearly all metrics, which proves that more proxies can effectively enhance and enrich the information of tail classes.

4 Conclusion

In this work, we present a class-enhancement contrastive learning framework, named ECL, for long-tailed skin lesion classification. Hybrid-proxy model and balanced-hybrid-proxy loss are proposed to tackle the problem that SCL-based methods pay less attention to the learning of tail classes. Class-dependent proxies are generated in hybrid-proxy model to enhance information of tail classes, where rich relations between samples and proxies are utilized to improve representation learning of the network. Furthermore, balanced-weighted cross-entropy loss is designed to help train an unbiased classifier by considering both "imbalanced data" and "imbalanced diagnosis difficulty". Extensive experiments on ISIC2018 and ISIC2019 datasets have demonstrated the effectiveness and superiority of ECL over other compared methods.

References

1. Ando, S., Huang, C.Y.: Deep over-sampling framework for classifying imbalanced data. In: Machine Learning and Knowledge Discovery in Databases: European Conference, ECML PKDD 2017, Skopje, Macedonia, September 18–22, 2017, Proceedings, Part I 10. pp. 770–785. Springer (2017)
2. Cao, K., Wei, C., Gaidon, A., Arechiga, N., Ma, T.: Learning imbalanced datasets with label-distribution-aware margin loss. *Advances in neural information processing systems* **32** (2019)
3. Cassidy, B., Kendrick, C., Brodzicki, A., Jaworek-Korjakowska, J., Yap, M.H.: Analysis of the isic image datasets: Usage, benchmarks and recommendations. *Medical image analysis* **75**, 102305 (2022)
4. Codella, N.C., Gutman, D., Celebi, M.E., Helba, B., Marchetti, M.A., Dusza, S.W., Kalloo, A., Liopyris, K., Mishra, N., Kittler, H., et al.: Skin lesion analysis toward melanoma detection: A challenge at the 2017 international symposium on biomedical imaging (isbi), hosted by the international skin imaging collaboration (isic). In: 2018 IEEE 15th international symposium on biomedical imaging (ISBI 2018). pp. 168–172. IEEE (2018)

5. Combalia, M., Codella, N.C., Rotemberg, V., Helba, B., Vilaplana, V., Reiter, O., Carrera, C., Barreiro, A., Halpern, A.C., Puig, S., et al.: Bcn20000: Dermoscopic lesions in the wild. arXiv preprint arXiv:1908.02288 (2019)
6. Esteva, A., Kuprel, B., Novoa, R.A., Ko, J., Swetter, S.M., Blau, H.M., Thrun, S.: Dermatologist-level classification of skin cancer with deep neural networks. *nature* **542**(7639), 115–118 (2017)
7. Hasan, M.K., Ahamad, M.A., Yap, C.H., Yang, G.: A survey, review, and future trends of skin lesion segmentation and classification. *Computers in Biology and Medicine* p. 106624 (2023)
8. He, K., Zhang, X., Ren, S., Sun, J.: Deep residual learning for image recognition. In: *Proceedings of the IEEE conference on computer vision and pattern recognition*. pp. 770–778 (2016)
9. Kang, B., Xie, S., Rohrbach, M., Yan, Z., Gordo, A., Feng, J., Kalantidis, Y.: Decoupling representation and classifier for long-tailed recognition. In: *International Conference on Learning Representations* (2019)
10. Khosla, P., Teterwak, P., Wang, C., Sarna, A., Tian, Y., Isola, P., Maschinot, A., Liu, C., Krishnan, D.: Supervised contrastive learning. *Advances in neural information processing systems* **33**, 18661–18673 (2020)
11. Lango, M., Stefanowski, J.: What makes multi-class imbalanced problems difficult? an experimental study. *Expert Systems with Applications* **199**, 116962 (2022)
12. Li, J., Chen, G., Mao, H., Deng, D., Li, D., Hao, J., Dou, Q., Heng, P.A.: Flat-aware cross-stage distilled framework for imbalanced medical image classification. In: *Medical Image Computing and Computer Assisted Intervention–MICCAI 2022: 25th International Conference, Singapore, September 18–22, 2022, Proceedings, Part III*. pp. 217–226. Springer (2022)
13. Li, T., Cao, P., Yuan, Y., Fan, L., Yang, Y., Feris, R.S., Indyk, P., Katabi, D.: Targeted supervised contrastive learning for long-tailed recognition. In: *Proceedings of the IEEE/CVF Conference on Computer Vision and Pattern Recognition*. pp. 6918–6928 (2022)
14. Lin, T.Y., Goyal, P., Girshick, R., He, K., Dollár, P.: Focal loss for dense object detection. In: *Proceedings of the IEEE international conference on computer vision*. pp. 2980–2988 (2017)
15. Marrakchi, Y., Makansi, O., Brox, T.: Fighting class imbalance with contrastive learning. In: *Medical Image Computing and Computer Assisted Intervention–MICCAI 2021: 24th International Conference, Strasbourg, France, September 27–October 1, 2021, Proceedings, Part III* 24. pp. 466–476. Springer (2021)
16. Menon, A.K., Jayasumana, S., Rawat, A.S., Jain, H., Veit, A., Kumar, S.: Long-tail learning via logit adjustment. In: *International Conference on Learning Representations* (2020)
17. Pouyanfar, S., Tao, Y., Mohan, A., Tian, H., Kaseb, A.S., Gaujen, K., Dailey, R., Aghajanzadeh, S., Lu, Y.H., Chen, S.C., et al.: Dynamic sampling in convolutional neural networks for imbalanced data classification. In: *2018 IEEE conference on multimedia information processing and retrieval (MIPR)*. pp. 112–117. IEEE (2018)
18. Tschandl, P., Rosendahl, C., Kittler, H.: The ham10000 dataset, a large collection of multi-source dermatoscopic images of common pigmented skin lesions. *Scientific data* **5**(1), 1–9 (2018)
19. Wang, P., Han, K., Wei, X.S., Zhang, L., Wang, L.: Contrastive learning based hybrid networks for long-tailed image classification. In: *Proceedings of the IEEE/CVF conference on computer vision and pattern recognition*. pp. 943–952 (2021)

20. Yang, L., Jiang, H., Song, Q., Guo, J.: A survey on long-tailed visual recognition. *International Journal of Computer Vision* **130**(7), 1837–1872 (2022)
21. Yao, P., Shen, S., Xu, M., Liu, P., Zhang, F., Xing, J., Shao, P., Kaffenberger, B., Xu, R.X.: Single model deep learning on imbalanced small datasets for skin lesion classification. *IEEE transactions on medical imaging* **41**(5), 1242–1254 (2021)
22. Zhou, B., Cui, Q., Wei, X.S., Chen, Z.M.: Bbn: Bilateral-branch network with cumulative learning for long-tailed visual recognition. In: *Proceedings of the IEEE/CVF conference on computer vision and pattern recognition*. pp. 9719–9728 (2020)
23. Zhu, J., Wang, Z., Chen, J., Chen, Y.P.P., Jiang, Y.G.: Balanced contrastive learning for long-tailed visual recognition. In: *Proceedings of the IEEE/CVF Conference on Computer Vision and Pattern Recognition*. pp. 6908–6917 (2022)

Supplementary Material: ECL: Class-Enhancement Contrastive Learning of Long-tailed Skin Lesion Classification

Table S1. Comparison results on ISIC2018 and ISIC2019 datasets. Data format: mean (standard deviation)

Methods	ISIC2018				
	Acc	Pre	Sen	F1	AUC
CE	83.89 (0.33)	69.56 (0.29)	73.62 (1.39)	70.34 (0.68)	94.81 (0.09)
Focal Loss	84.19 (0.13)	68.78 (0.43)	76.69 (0.48)	71.38 (0.41)	94.76 (0.02)
LDAM-DRW	84.20 (0.09)	71.74 (0.43)	74.65 (0.26)	71.98 (0.32)	95.22 (0.05)
Logit Adjust	84.15 (0.27)	71.54 (1.30)	71.78 (1.10)	70.77 (0.04)	95.55 (0.04)
MWNL	84.90 (0.20)	73.90 (0.43)	76.94 (0.35)	74.92 (0.43)	96.79 (0.14)
BBN	85.57 (0.40)	74.96 (1.23)	72.40 (2.75)	72.79 (1.02)	93.72 (0.03)
Hybrid-SC	86.30 (0.36)	73.93 (0.46)	75.84 (4.48)	74.34 (2.13)	96.33 (0.53)
SCL	86.13 (0.22)	70.40 (0.91)	80.88 (0.97)	74.27 (0.86)	96.56 (0.08)
BCL	84.92 (0.49)	72.87 (0.85)	71.15 (0.66)	71.57 (0.51)	95.61 (0.10)
TSC	85.94 (0.46)	73.35 (1.80)	77.77 (1.60)	74.94 (1.66)	95.83 (0.19)
Ours	87.20 (0.12)	73.01 (0.48)	83.44 (0.77)	76.76 (0.33)	96.55 (0.03)
Methods	ISIC2019				
	Acc	Pre	Sen	F1	AUC
CE	82.41 (0.19)	67.02 (0.10)	77.32 (0.25)	70.90 (0.10)	95.37 (0.04)
Focal Loss	82.05 (0.11)	64.55 (0.20)	75.93 (0.90)	68.84 (0.31)	94.82 (0.04)
LDAM-DRW	82.29 (0.10)	68.08 (0.34)	74.61 (0.12)	70.84 (0.23)	95.65 (0.02)
Logit Adjust	81.93 (0.21)	68.94 (0.29)	69.12 (0.14)	68.64 (0.21)	95.17 (0.01)
MWNL	84.10 (0.18)	74.83 (0.78)	75.81 (0.52)	75.08 (0.23)	96.61 (0.04)
BBN	83.43 (0.10)	71.78 (1.32)	78.37 (2.18)	74.42 (0.33)	95.10 (0.07)
Hybrid-SC	84.69 (0.09)	70.90 (0.38)	76.87 (0.25)	73.27 (0.38)	96.67 (0.04)
SCL	84.60 (0.24)	70.90 (1.57)	81.66 (0.54)	75.07 (1.23)	96.21 (0.07)
BCL	83.47 (0.10)	73.52 (1.40)	74.17 (1.12)	73.50 (0.29)	95.95 (0.03)
TSC	84.75 (0.15)	71.89 (0.64)	79.81 (0.31)	75.13 (0.32)	95.84 (0.03)
Ours	86.11 (0.16)	76.57 (0.94)	83.22 (0.10)	79.46 (0.58)	96.78 (0.09)

Table S2. Ablation study on ISIC2018 and ISIC2019 datasets. Data format: mean (standard deviation)

Methods(ISIC2018)	Proxies	Acc	Sen	Pre	F1	AUC
Classifier branch-CE	HPM	83.89 (0.33)	69.56 (0.29)	73.62 (1.39)	70.34 (0.68)	94.81 (0.09)
Classifier branch-BWCE	HPM	84.83 (0.44)	70.13 (1.85)	77.38 (0.46)	72.28 (1.33)	94.94 (0.16)
Dual branch-CE+BHP	HPM	86.78 (0.18)	72.96 (0.21)	81.73 (0.21)	76.05 (0.97)	96.74 (0.08)
Dual branch-BWCE+BHP w/o cycle update strategy	HPM	86.43 (0.09)	72.42 (0.56)	81.32 (0.26)	75.14 (0.18)	96.50 (0.02)
Dual branch-BWCE+BHP	2 proxies per-class	86.33 (0.26)	71.32 (0.80)	81.86 (1.41)	75.18 (0.68)	96.30 (0.09)
Dual branch-BWCE+BHP	3 proxies per-class	86.36 (0.28)	70.47 (1.21)	82.20 (0.54)	74.70 (0.75)	96.59 (0.06)
Dual branch-BWCE+BHP	4 proxies per-class	86.45 (0.33)	71.54 (0.52)	80.54 (2.00)	75.84 (0.44)	96.66 (0.04)
Dual branch-BWCE+BHP	HPM	87.20 (0.12)	73.02 (0.48)	83.44 (0.77)	76.76 (0.33)	96.55 (0.03)
Methods(ISIC2019)	Proxies	Acc	Sen	Pre	F1	AUC
Classifier branch-CE	HPM	82.41 (0.19)	67.02 (0.10)	77.32 (0.25)	70.90 (0.10)	95.37 (0.04)
Classifier branch-BWCE	HPM	82.69 (0.14)	67.95 (0.77)	77.32 (0.31)	71.65 (0.46)	95.35 (0.03)
Dual branch-CE+BHP	HPM	85.49 (0.03)	73.35 (0.30)	81.61 (0.30)	76.76 (0.31)	96.52 (0.03)
Dual branch-BWCE+BHP w/o cycle update strategy	HPM	85.65 (0.48)	73.48 (0.48)	83.00 (1.60)	77.40 (0.60)	96.65 (0.15)
Dual branch-BWCE+BHP	2 proxies per-class	85.52 (0.03)	74.03 (0.28)	81.46 (0.12)	77.22 (0.13)	96.53 (0.03)
Dual branch-BWCE+BHP	3 proxies per-class	85.36 (0.09)	73.49 (0.10)	83.00 (0.33)	77.53 (0.20)	96.74 (0.02)
Dual branch-BWCE+BHP	4 proxies per-class	85.79 (0.03)	74.09 (0.62)	82.03 (0.66)	77.42 (0.56)	96.53 (0.03)
Dual branch-BWCE+BHP	HPM	86.11 (0.16)	76.57 (0.94)	83.22 (0.06)	79.46 (0.58)	96.78 (0.09)